*Ann. Rev. Earth Planet. Sci. 1980. 8:489–525*


# FRACTURE MECHANICS APPLIED TO THE EARTH'S CRUST



*John W. Rudnicki*
Department of Theoretical and Applied Mechanics, University of Illinois, Urbana, Illinois 61801

## INTRODUCTION

Fracture mechanics concerns the study of stress concentrations caused by sharp-tipped flaws and the conditions for the propagation of these flaws. Although this approach has been very successful at explaining many features of the brittle and ductile failure of technological materials (metals, ceramics, glasses, polymers) under tensile loads, its application to geophysics has not been widespread. This is due, at least in part, to a historical preference for an approach that employs results from the theory of dislocations in elastic solids. With regard to the analysis of the stress or displacement induced by relative displacement on a surface of discontinuity, the two approaches are essentially coincident. They differ, however, with respect to the criteria for growth or spreading of the surface of discontinuity. In the dislocation approach, the relative motion on the surface of discontinuity is assumed a priori whereas, in fracture mechanics, a criterion based on plausible physical grounds or experimental evidence is used to determine whether the region of relative displacement will spread. The usefulness of the fracture mechanics approach is largely due to the success of simple fracture criteria in describing the failure of many materials. This article will focus on fracture criteria for the earth's crust.

The reluctance to adopt the fracture mechanics approach may also be due, in addition to historical reasons, to the attitude that so little is known about the details of the failure process in the earth's crust that the pursuit of studies based on assuming a fracture criterion is not worthwhile. There is, of course, good reason for this objection: seismological data is typically collected at large distances from the faults and is complicated by propagation effects; geological data is mostly limited to the earth's surface and is often obtained a long time after faulting occurs; and experimental data



0084-6597/80/0515-0489$01.00

is limited to size and time scales vastly different from those in situ. Moreover, seismologists have been very successful in using simple dislocation models to describe the transient motion due to earthquakes. In spite of these difficulties, the increasing sophistication of seismic studies of the transient motion near earthquake sources (strong motion studies; see, for example, Heaton & Helmberger 1978) and the direct observation of medium scale faulting in mines (McGarr et al 1979) suggest that these studies can be used with experimental and theoretical work to obtain a better understanding of failure processes in the earth's crust. Indeed, even an elementary understanding of the vast variety of earthquake-related phenomena, foreshocks, swarms, fault creep, aftershocks, etc. seems impossible without better knowledge of a fracture criterion.

The next section will review the fundamentals of fracture mechanics and discuss some aspects of fracture criteria. Although fracture mechanics has developed to the point where several texts (Knott 1973, Broek 1974, Lawn & Wilshaw 1975)[1] as well as extensive treatises (Liebowitz 1968) are available, some of the essential ideas are not well understood. The relationship between models that idealize the crack-tip as a singular stress field and those that include a cohesive zone will be discussed. In particular, the application of the Palmer & Rice (1973) cohesive zone model to shear faulting will be discussed in detail. Succeeding sections will review data from laboratory experiments, including some recent experiments on stress corrosion cracking in rock, and data inferred from observations of crustal faulting. Some results for fracture propagation in viscoelastic and fluid-infiltrated solids will be reviewed and the implications of these studies for fault creep and migration of seismic activity will be discussed. Finally, some aspects of rupture in the earth's crust, which are not possible to treat within the present framework of fracture mechanics, will be mentioned. Freund (1979) has recently reviewed several aspects of dynamic fracture mechanics relevant to fault propagation. Consequently, in this article inertial effects will, for the most part, be neglected and any growth of the fracture will be assumed to take place quasi-statically.

## FUNDAMENTALS OF FRACTURE MECHANICS

### *Linear Elastic Crack-Tip Stress Fields*

Consider a body which is infinite in extent in one direction (plane strain conditions) and which, except for the presence of the crack, is linearly elastic, isotropic, and homogeneous. The stresses near the crack-tip then

[1] Because these texts and treatises are available, no effort will be made to reference the original source when citing a result from fracture mechanics.

have the following form [e.g. Rice 1968a, Equations (78–83)]:

$$\sigma_{ij} = K_L(2\pi r)^{-1/2} f_{ij}^L(\theta) + O(1) \quad (L = I, II, III), \tag{1}$$

where $r$ is the distance from crack-tip, $\theta$ is the angle measured from the plane ahead of the crack, and $O(1)$ denotes terms which are bounded at the crack-tip. The coefficients $K_L$ are the stress intensity factors and the index L refers to the type of loading: loading which tends to cause separation of the crack faces is designated as mode I; loading which tends to cause relative slip is called mode II (plane strain shear) or mode III (anti-plane shear) depending on whether the slip is perpendicular or parallel to the crack edge. The functions $f_{ij}(\theta)$ are the same for all loadings of a given type (mode I, II, or III) and, thus, all details of the geometry and applied loading are contained in $K$. The stress intensity factor is proportional to the magnitude of the applied loading and to the square root of a characteristic length.

As examples of specific forms for the stress intensity factor, consider the mode II loadings, which are shown in Figure 1, and which have been discussed by Rice & Simons (1976). In Figure 1*a* a crack of length $l$ is loaded at infinity by uniform shear stresses $\tau_\infty$. If the crack encloses no net dislocation so that the displacement field is single-valued outside the fault, the stress intensity factor is (Paris & Sih 1965)

$$K_{II} = \tau_\infty(\pi l/2)^{1/2}. \tag{2}$$

If there is an entrapped dislocation of magnitude sufficient to eliminate the singularity at one end of the crack, the stress intensity factor at the

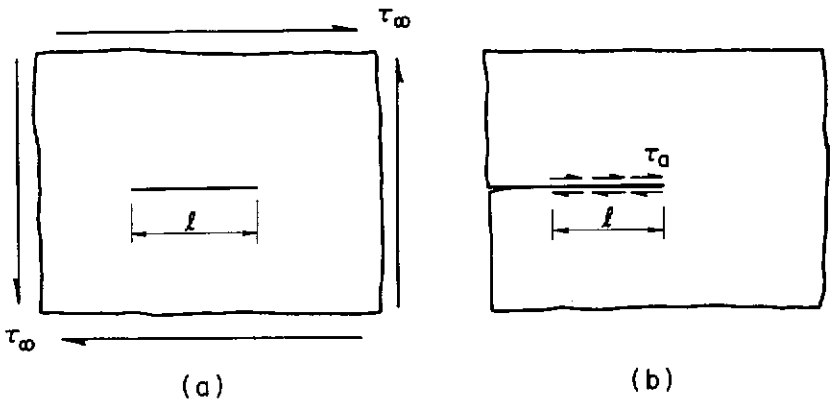


*Figure 1* (*a*) Frictionless shear fault idealized as mode II crack. (*b*) Shear fault idealized as a semi-infinite mode II crack loaded by effective stress $\tau_a$ applied to a length $l$ of the crack surfaces.

other end is [Rice 1968a, Equation (318)]

$$K_{II} = \tau_\infty (2\pi l)^{1/2}. \tag{3}$$

If the crack models a fault that has a resistive frictional stress $\tau_f$, then appropriate values for $K_{II}$ are given by Equations (2) and (3) with the difference $\tau_\infty - \tau_f$ replacing $\tau_\infty$. Often the analysis is simplified by treating a crack or fault as semi-infinite with loading applied over a finite portion of the surface, as illustrated in Figure 1*b*. The stress intensity factor for this geometry is [Rice 1968a, Equation (98)]

$$K_{II} = \tau_a (8l/\pi)^{1/2} \tag{4}$$

where $\tau_a$ may again be chosen as the excess of a remote stress over the fault friction. The length over which the loading is applied can be adjusted so that stresses near the fault-tip are the same as those in Figure 1*a*.

There is a large number of solutions for crack problems of various loadings and geometries (Paris & Sih 1965, Tada, Paris & Irwin 1973) and these provide a powerful means of stress analysis near faults and other acute geometries. The solutions in the form of (1) pertain strictly to plane strain conditions, but it is evident that such conditions are approached asymptotically near the edge of a crack in a three-dimensional body. Kassir & Sih (1966) verified this result directly for elliptical cracks and it is likely to apply for all cracks for which the edge has a smoothly turning tangent. The number of three-dimensional solutions is somewhat limited, but Weaver (1977) has recently presented an expedient numerical procedure for solving three-dimensional crack problems and has used it to study stresses near the edge of a rectangular fault [Budiansky & Rice (1979) have extended this procedure to dynamic problems].

The stresses near the crack-tip, as given by Equation (1), exhibit the characteristic $r^{-1/2}$ singularity of linear elastic fracture mechanics. Stresses which are more singular than these (for example, the stresses near a straight dislocation line are proportional to $r^{-1}$) are prohibited by requiring that the strain energy be finite in any bounded volume enclosing the crack-tip. Of course, in any real material, the high stresses near the crack-tip will be alleviated by inelastic deformation which accompanies the micromechanical processes of separation or relative sliding. If, however, this "process zone" has a characteristic length that is much less than other length scales in the problem (e.g. crack or fault length, distance to boundaries, etc.), then the conditions at the boundary of this zone are fixed by the surrounding linear elastic field and, in this sense, the intensity of deformation within this region is characterized by the stress intensity factor. When these so-called small scale yielding conditions (Rice 1968a, b) prevail, it is possible to ignore the details of inelastic processes near the

crack-tip, which are often poorly known, and to treat the problem as fully elastic with the understanding that $K$ characterizes the actual near tip field. Conversely, a boundary layer formulation (Rice 1968b, Edmunds & Willis 1976, Simons 1977) may be employed to study the details of the near-tip region for more realistic material models by imposing the condition that the deformation field approach the elastic solution as distance from the crack-tip becomes large.

## *Relation to Elastic Dislocations*

In geophysics, a more popular approach to stress analysis near faults has made use of the theory of dislocations in elastic solids (e.g. Steketee 1958). Although this approach may be intuitively appealing to some because it reflects more directly the notion of idealizing faulting as slip on a planar surface, it is essentially equivalent to the approach taken in fracture mechanics. To illustrate this equivalence, consider a straight edge dislocation at a point $x = \xi$ on the axis $y = 0$ with a Burger's vector $b$ in the $x$ direction. The shear stress on the $x$ axis is given by

$$\tau_d = \mu b/[2\pi(1-\nu)(x-\xi)] \tag{5}$$

where $\nu$ is Poisson's ratio and $\mu$ is the shear modulus. If there is a continuous distribution of dislocations with infinitesimal Burger's vectors over a segment $S$ of the $x$ axis, then the resulting stress is

$$\tau_d = \frac{\mu}{2\pi(1-\nu)} \int_S \frac{B(\xi)}{x-\xi}\, d\xi \tag{6}$$

where $B(\xi) = -\partial b/\partial \xi$ is the dislocation density. If $S$ is assumed to represent a fault with resistive stresses $\tau(x)$ applied to the fault surfaces and a constant stress $\tau_\infty$ applied remotely, then the condition

$$\tau(x) = \tau_\infty + \tau_d \tag{7}$$

yields an integral equation for determining $B(\xi)$. As an example, consider the special case in which $\tau(x) = \tau_f$, a constant, as for the configuration shown in Figure 1*a*. If the crack encloses no net dislocation, $B(\xi)$ satisfies the condition [Equation (115) in Rice (1968a)]

$$\int_{-l/2}^{l/2} B(\xi)\, d\xi = 0, \tag{8}$$

and, in this case, the solution of (7) is

$$B(\xi) = 2\mu^{-1}(1-\nu)(\tau_\infty - \tau_f)\, \xi[(l/2)^2 - \xi^2]^{-1/2}. \tag{9}$$

The relative displacement of the fault surface is

$$\delta(x) = 2\mu^{-1}(\tau_\infty - \tau_f)[(l/2)^2 - x^2]^{1/2}, \tag{10}$$

but this can, of course, be determined by other methods [for example, see Equations (22) and (96) of Rice (1968a)].

A thorough discussion of this method has been given by Bilby & Eshelby (1968). This approach is often advantageous when $S$ is regarded as a frictional surface and the stress sustained by the surface is related nonlinearly to the relative slip on the surface (e.g. Cleary 1976, Rudnicki 1979, Stuart & Mavko 1979). However, when the stress on $S$ is regarded as given, these problems can often be solved more directly by other techniques (Rice 1968a). Alternatively, the stress on the fault may be regarded as unknown and chosen to satisfy some other condition in the problem. For example, Dmowska (1973) and Freund & Barnett (1976) have used this procedure to estimate the distribution of stress on dip-slip faults [Barnett & Freund (1975) treated the strike-slip case] by comparing calculated with observed surface displacements.

## *Energy Release Rate*

During an infinitesimal increase in the length of a crack in a linearly elastic body, the work done by the tractions on any contour surrounding the crack-tip exceeds the increase of strain energy of the material within the contour. This difference, denoted $G$, is the energy released per unit area of crack advance. If the boundary displacements are fixed during the crack advance then $G$ equals the *decrease* of potential energy per unit crack advance. Rice (1966) has shown that $G$ can also be calculated as the work which is done in unloading the newly created crack surfaces. Because the near-tip stress field has the universal form (1) in a linearly elastic solid, $G$ can be expressed in terms of the stress intensity factors as

$$G = [K_{\mathrm{I}}^2 + K_{\mathrm{II}}^2 + K_{\mathrm{III}}^2(1-\nu)^{-1}](1-\nu)(2\mu)^{-1} \tag{11}$$

for any combination of plane strain and anti-plane shear loadings. Consequently, for small scale yielding conditions, $G$ is an alternative to $K$ as a parameter that characterizes the intensity of the near-tip deformation. However, as Rice (1966, 1979a) has emphasized, it is implicit in (11) that the energy release can be calculated from the elastic singularity independently of the actual microstructural breakdown processes. In other words, in this purely continuum viewpoint the release of energy is due to the motion of the singularity in the elastic stress field which accompanies crack advance.

A viewpoint that has proved to be extremely useful is that extension of the fracture occurs when $G$ is equal to some critical value, say $G_{\mathrm{crit}}$. In the

case of purely brittle fracture considered by Griffith (1920), $G_{crit} = 2\Gamma_0$ where $\Gamma_0$ is the specific surface energy. More generally, however, $G_{crit}$ may be taken to represent the energy required for the microstructural processes of breakdown near the crack-tip. Thus, the fracture criterion is

$$G = G_{crit}. \tag{12}$$

Because of (11), it is clear that the criterion (12) is equivalent to the condition that fracture occurs, for a given type of loading, when the stress intensity factor attains some critical value. Although this criterion is very simple, it often is an improvement over other simple criteria that are commonly used. For example, Abou-Sayed, Bretchel & Clifton (1978) employed the fracture criterion (12) in a study of stress determination by hydraulic fracturing. They concluded that the maximum horizontal stress was overestimated by an analysis based on a maximum tensile stress criterion because the effect of loading the faces of pre-existing cracks was neglected.

It is worth repeating that the left-hand side of (12) is determined by a calculation which assumes that the crack-tip can be idealized as a singularity in the elastic stress field whereas the right-hand side is determined from a model which makes more detailed assumptions about the nature of processes at the crack-tip. Such an uncoupling is not always realistic. Indeed, Rice (1979a) has stressed that all attempts to use such an approach as a fracture criterion for inelastic solids have led to physically unacceptable results. (Examples relevant to geophysics will be given in a subsequent section.)

## *J Integral*

Another useful tool in fracture mechanics is the $J$ integral which was first applied extensively to fracture mechanics by Rice (1968b) although Cherepanov (1968) and Eshelby (1956) had earlier introduced similar integrals. For a coordinate system chosen so the crack line coincides with the $x$ direction and the $y$ direction is perpendicular to the crack surface, the $J$ integral is defined as (Rice 1968b)

$$J = \int_C (W n_x - n_i \sigma_{ij} \partial u_j / \partial x)\, ds \qquad (i,j = x,y) \tag{13}$$

where $\sigma_{ij}$ and $u_j$ are the stress and displacement components, respectively;

$$W(\varepsilon_{ij}) = \int_0^{\varepsilon_{ij}} \sigma_{ij}\, d\varepsilon'_{ij} \tag{14}$$

is the strain energy density; $s$ is the arc length and the $n_i$ are the com-

ponents of the unit normal to the contour $C$ which begins and ends on the crack surfaces and encloses the crack-tip. Generalizations of this integral have been discussed by Eshelby (1970), Knowles & Sternberg (1972), and Budiansky & Rice (1973).

The utility of $J$ arises from the fact that it is path-independent in linear or nonlinear elastic materials which are homogeneous in the $x$ direction (Rice 1968b). [If the crack surfaces are not traction-free, the value of $J$ does depend on the endpoints but is the same for all paths with the same endpoints (Palmer & Rice 1973).] Thus, evaluation of $J$ on a remote contour and one near the crack-tip makes it possible to relate conditions at the crack-tip to parameters characterizing the applied loads. (An example of the application of $J$ will be given later.) Moreover, in the case of small scale yielding, Rice (1968b; see also Palmer & Rice 1973) has shown that $J$ is equal to the energy release rate $G$. Thus, for small scale yielding, $J$, in addition to $G$, is an alternative to $K$ as a parameter that characterizes the intensity of the near-tip deformation. Indeed, it is a feature of linear elastic fracture mechanics that a single parameter, of which $J$, $G$, and $K$ are three possibilities, characterizes the near-tip field. $J$, however, has the additional advantage of possessing a precise meaning for nonlinearly elastic behavior (or for time-independent inelastic behavior if unloading is not allowed) and, thus, there is the possibility of using $J$ to correlate experiments in which substantial amount of inelasticity occurs.

## *Cohesive Force Models for Shear Faulting*

The microstructural processes of breakdown near the crack-tip can be included directly by assuming that they give rise to cohesive forces in a zone ahead of the crack-tip. These forces oppose the action of the applied loads so as to eliminate the crack-tip singularity. Several cohesive force models have been suggested for tensile cracks (Barenblatt 1962, Dugdale 1960, Bilby, Cottrell & Swindon 1963) and Ida (1972) has proposed a cohesive force model for steady propagation of an anti-plane shear fault. However, treatment here will follow the formulation proposed by Palmer & Rice (1973), hereafter abbreviated as PR, for shear band propagation in clay slopes and applied by Rice (1979b) and by Rice & Simons (1976) to shear faulting.

The PR model is shown schematically in Figure 2. In Figure 2*a*, $\tau_f$ is the residual friction stress on the fault surface, but the stress rises to $\tau_p$ near the end of the fault because of microstructural processes which cause resistance to slip initiation. In Figure 2*b*, the stress on the fault surface is shown as a function of the relative sliding $\delta(x)$. An amount of sliding $\delta^*$ is necessary to reduce $\tau_p$ to $\tau_F$. In general, the end zone size is not known

a priori. If, however, the end zone is small (small scale yielding), then its length can be determined by requiring the cohesive forces to cancel the singularity that would be caused by the applied loads in the absence of the end zone. As an example, consider the semi-infinite fault in Figure 1*b* with a small end zone and a constant distribution (Figure 3*a*) of stress in the end zone. The end zone size is given by [see Equation (10) of Rice & Simons (1976) and Equation (44) of PR]

$$R = \pi K^2 [8(\tau_p - \tau_f)^2]^{-1} \tag{15}$$

where $l$ in Figure 1*b* is the total length over which the loads are applied (including the end zone), and $K$ is the stress intensity factor caused by the applied loads in the absence of the end zone. Because $K$ for this geo-

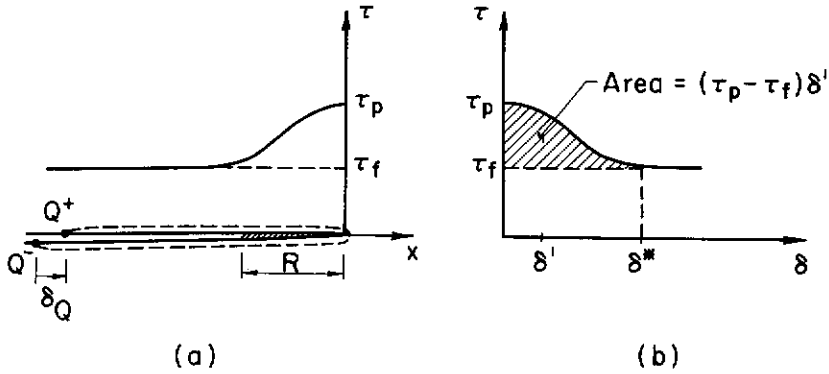


*Figure 2* Palmer & Rice (1973) model of a cohesive zone. (*a*) Fault surface stress as a function of distance back from the fault-tip. Dashed line denotes contour for $J$ integral used in deriving Equation (20). (*b*) Fault surface stress as a function of relative slip on the fault.

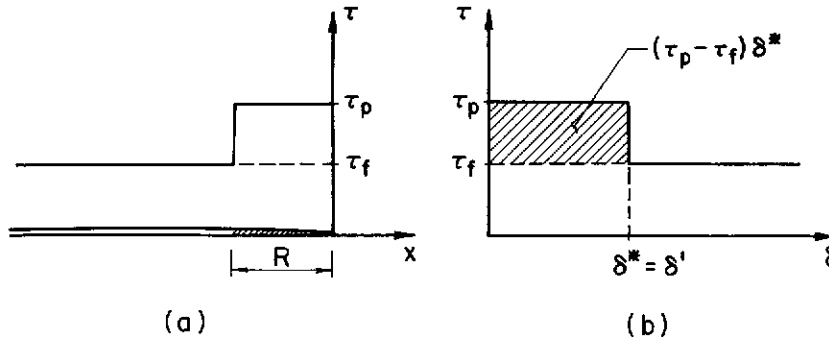


*Figure 3* Palmer & Rice (1973) cohesive zone model with constant end zone stress.

metry is given by (4), Equation (15) can be rewritten as

$$R = l[(\tau_\infty - \tau_f)/(\tau_p - \tau_f)]^2. \tag{16}$$

If the stress in the end zone decreases linearly from $\tau_p$ to $\tau_f$, instead of being constant, the expressions in (15) and (16) should be multiplied by 9/4. The relative slip in the end zone can be obtained by a standard calculation of fracture mechanics (Rice 1968a). For a small end zone, the result can be expressed as

$$\delta(x) = (1-\nu) K^2 f(|x|/R)[2\mu(\tau_p - \tau_f)]^{-1} \tag{17}$$

where $f(0) = 0$ and $f(1) = 1$ and, for the case of constant end zone stress

$$f(\lambda) = \lambda^{1/2} - \tfrac{1}{2}(1-\lambda) \log [(1+\lambda^{1/2})/|1-\lambda^{1/2}|]. \tag{18}$$

A fracture criterion which is appropriate for this model is that fault growth occurs when the relative displacement at the end of the breakdown zone is sufficient to reduce $\tau_p$ to $\tau_f$ or, more concisely, when

$$\delta(x = -R) = \delta^*. \tag{19}$$

The work expended in accomplishing this reduction, in excess of the work done against friction $\tau_f$, is simply the shaded area in Figure 2*b* (or Figure 3*b* for constant end zone stress). As demonstrated by PR, this work can be expressed in terms of the $J$ integral by evaluating Equation (13) on a contour along the fault surfaces as shown in Figure 2*a*. The result is [PR, Equation (7)]

$$J_Q - \tau_f \delta_Q = \int_0^{\delta(x=-R)} (\tau - \tau_f)\, d\delta \tag{20}$$

where $Q$ denotes the position of the contour endpoints (assumed to be outside the end zone) and $\delta_Q$ is the relative slip of the fault surfaces at $Q$. [Note that $n_x = 0$ for this contour so that only the second term under the integral in (13) contributes to (20). The form of (20) then results from recognizing that in the end zone $\tau$ is a single-valued function of $\delta$.] When (19) is satisfied, the right-hand side of (20) can be recognized as the shaded area in Figure 2*b* where $\delta'$ is defined by the relation

$$(\tau_p - \tau_f)\delta' = \int_0^{\delta^*} [\tau(\delta) - \tau_f]\, d\delta. \tag{21}$$

The right side of (21) is the work that is necessary to overcome the cohesive forces and advance the fracture. For a vanishingly small end zone this work *defines* the critical value of the energy release rate,

$$(\tau_p - \tau_f)\delta' = G_{crit}, \tag{22}$$

and, in this small end zone case, the Griffith criteria of Equation (12) for a singular crack-tip model is equivalent to the criteria expressed by (19) for a cohesive zone model. Willis (1967) first demonstrated this equivalence by a direct calculation based on complex variable methods and Rice (1968b) confirmed the result using the $J$ integral. Formally, the equivalence can be rationalized by reducing the end zone size to zero while allowing $\tau_p - \tau_f$ to become unbounded in a manner such that the right-hand side of (21) remains finite and equal to $G_{crit}$. The size of the breakdown zone $R$ can now be expressed in terms of $\delta'$ by using Equation (11) (with $K = K_{II}$ and $K_I = K_{III} = 0$) and Equation (22) in Equation (15). The result is

$$R = \pi\mu\delta'[4(\tau_p - \tau_f)(1-\nu)]^{-1}. \tag{23}$$

Cohesive zone models have been widely used in studies of dynamic fault propagation (e.g. Ida 1973a, Andrews 1976a,b, Das & Aki 1977a,b) because they avoid the numerical difficulties associated with treating a singular crack-tip stress field. In the case of dynamic crack propagation, the Griffith fracture criteria (based on an energy balance at the tip of a crack at which stress is singular) is not, however, exactly equivalent to a criteria based on the achievement of a certain relative displacement in the end zone [as expressed, for example, by Equation (19)] even if the end zone is small. As Freund (1976a, 1979) has emphasized, the two criteria are equivalent for small end zones only if, in addition, conditions are completely steady as viewed by an observer moving with the crack tip. Because results are more dependent on the choice of fracture criteria than in the quasi-static case, it is often difficult to distinguish general features of the solution from those which are peculiar to the particular model and method of discretization. Ida (1972) introduced a cohesive zone model for dynamic propagation of a mode III crack and he considered several forms for the decrease of stress with relative slip in the cohesive zone. His treatment was, however, limited to steady state conditions and small end zones. Andrews (1976a,b) studied the propagation of anti-plane strain and plane strain shear faults for a cohesive zone model in which the stress decreased linearly with slip. For plane strain fault propagation (Andrews 1976b), he found that the propagation speed could exceed the Rayleigh wave velocity, in contrast to predictions based on singular crack-tip models. The study of Das & Aki (1977a) is purportedly based on the criterion that propagation occurs when the dynamic stress intensity factor attains a certain level. The result of the discretization is, however, a criterion that requires that a certain stress level be achieved over a critical length. Freund (1979) has given an example demonstrating that predictions based on this criterion differ from those based on a critical value of the stress intensity factor. In the discretized fracture criterion of Das & Aki (1977a) the

critical distance has no apparent physical basis and is simply identified as the grid spacing in the finite difference calculation. Das & Aki (1977b) used this criterion in the study of fault propagation on a plane with barriers, that is, areas of the fault plane where the critical stress level was locally higher. One of their results is the prediction that the propagating fault can leave areas behind the tip on which no relative slip occurs. In the absence of a physical basis for the critical length in the fracture criterion, it is, however, impossible to evaluate whether the predictions of this model are realistic.

## EXPERIMENTAL VALUES OF MATERIAL PARAMETERS

### *Experimental Determination of $K_{IC}$*

If any inelastic behavior near the tip of a crack is confined to a sufficiently small region and if the onset of crack growth is unstable (i.e. results in abrupt loss of load bearing capacity), then the value of the crack-tip stress intensity factor at fracture may be identified as a material parameter characterizing failure. For tensile (mode I) loading this critical value of $K$ is usually denoted $K_{IC}$. Because of the success of linear elastic fracture mechanics in describing the brittle failure of technological materials, much attention has been given to establishing standard experimental procedures for measuring $K_{IC}$. There have recently been attempts to apply these procedures to the determination of $K_{IC}$ for rocks and an ASTM subcommittee (E24.07) on the Fracture Testing of Brittle Non-metallic Materials was formed in 1977. Although $K_{IC}$ has obvious relevance for tensile fracture as, for example, in hydraulic fracturing (Abou-Sayed, Brechtel & Clifton 1978), there may be some question about the applicability of these results to shear faulting. The macroscopic inelastic behavior of brittle rock does, however, result from microcracking at the tips of pre-existing fissures where the stress fields can be locally tensile even when all the applied principal stresses are compressive (Tapponnier & Brace 1976, Kranz 1979a,b). Macroscopic shear failure appears, at least in laboratory experiments, to result from the rapid growth and link-up of these fractures and the direct observation of fracture surfaces associated with seismic events in mines (McGarr et al 1979) suggests that this process may be prevalent on a larger scale. At the very least, studies of $K_{IC}$ are likely to improve the understanding of inelastic processes and fracture in rocks.

Investigators have measured $K_{IC}$ for a variety of rocks using a number of different tests (Clifton et al 1976, Abou-Sayed 1977, Abou-Sayed, Brechtel & Clifton 1978, Kobayashi & Fourney 1978, Schmidt 1976, 1977, Schmidt & Huddle 1977, Schmidt & Lutz 1979, Atkinson 1979a) and

Atkinson (1979a) has tabulated many of the existing results. Most of the rocks tested were carbonates or sandstones and a representative value of $K_{IC}$ seems to be 1 $MNm^{-3/2}$. Schmidt & Huddle (1977) have, however, found that $K_{IC}$ for Indiana limestone increased with confining pressure from 930 $kNm^{-3/2}$ at atmospheric pressure to 4.20 $MNm^{-3/2}$ at 62 MPa. Measurements of $K_{IC}$ for granite have been less frequent: Schmidt & Lutz (1979) obtained a preliminary value of 2.5 $MNm^{-3/2}$ for Westerly granite whereas Atkinson & Rawlings (1979a) and Swanson & Spetzler (1979) reported a lower value of 1.74 $MNm^{-3/2}$. Atkinson (personal communication, 1979) has also obtained $K_{IC} = 1.66$ $MNm^{-3/2}$ for a "coarse orthoclase feldspar granite" and Atkinson & Rawlings (1979b) obtained $K_{IC} = 2.9$ $MNm^{-3/2}$ for a gabbro. These values of $K_{IC}$ can be converted to critical values of the energy release rate by using Equation (11) with $K_{II} = K_{III} = 0$. For $\mu = 20$ GPa (1 GPa = $10^9$ $Nm^{-2}$ = $10^4$ bars) and $\nu = 0.2$, $K_{IC}$ values of 1, 2.5, and 4 $MNm^{-3/2}$ yield $G_{crit} = 20$, 125, and 320 J $m^{-2}$, respectively.

In the testing of metals, an empirical criterion that ensures that the inelastic zone at the crack-tip is sufficiently small has been found to be (Brown & Srawley 1966)

$$\text{crack length} > 2.5\,(K_I/\sigma_y)^2 \tag{24}$$

where $\sigma_y$ is the yield stress (the stress at which the first departure from linearly elastic behavior occurs). If this condition is met, the value of $K_I$ may be identified as the material parameter $K_{IC}$. This criterion seems to apply approximately in brittle rocks when the ultimate (peak) stress $\sigma_u$ is substituted for $\sigma_y$. However, the right-hand side of (24) is based on a formulation for metal plasticity and because the inelasticity of brittle rocks results primarily from microcracking rather than dislocation motion, this criterion may not be appropriate. For a crack in a 12.9-mm-thick plate of Westerly granite, Kobayashi & Fourney (1978) observed thin cracks extending 13 mm and 20 mm ahead of the main crack when the applied value of $K_I$ was 660 $kNm^{-3/2}$ and 990 $kNm^{-3/2}$, respectively. For $\sigma_u =$ 21 MPa (Jaeger & Cook 1976, Brace 1964), using $(K/\sigma_u)^2$ as an estimate for the size of the inelastic zone yields values too small by a factor of 10. A clear interpretation is prevented by the fact that the thinness of the plate is likely to have caused departure from plane strain conditions.

Wilkening (1978) has suggested that measurements of $K_{IC}$ may be invalid because a significant amount of stable crack growth occurs prior to fracture. Consequently, he has employed the $J$ integral, which may be applied in situations of inelastic loading, if unloading is not permitted, as a parameter characterizing conditions at fracture. On the basis of his direct measurements of $J$ for Barre granite, Wilkening (1978) concluded that

calculations of $J$ based on linear elasticity and the identity $J = G$ for small end zones underestimate the actual value by a factor of 2 to 3. On the other hand, Schmidt & Lutz (1979) found that measurements of $K$ and $J$ for Westerly granite were generally in agreement. Unfortunately, there are not enough data available to resolve these differences but, given the nonlinear behavior of rock prior to fracture, more direct measurements of $J$ would seem to be a worthwhile underatking.

## *Stress Corrosion Cracking*

It is well known that the presence of water or other pore fluid in either liquid or vapor form can enhance microcrack growth in brittle rocks (e.g. Martin 1972, Scholz 1972, Swolfs 1972, Martin & Durham 1975, Anderson & Grew 1977). In particular, surface chemical effects can cause slow stable crack growth at values of the applied stress intensity factor ($K_I$) which are well below the critical value for unstable growth ($K_{IC}$). Such time-dependent crack growth has been observed in glass and ceramics (see Wachtman 1974 for a review), but only a few detailed results exist for rock. The results for glass and ceramics are often summarized in a logarithmic plot of crack velocity ($V$) versus the applied stress intensity factor ($K_I$) such as that shown schematically in Figure 4. Slow crack growth in region I is thought to be controlled by surface chemical effects. In region

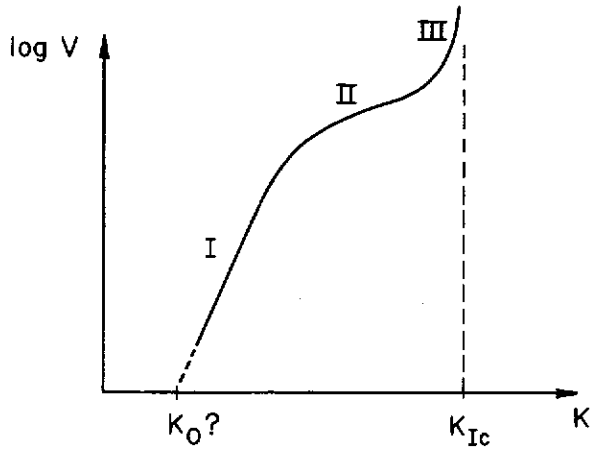


*Figure 4* Schematic illustration of typical results on stress corrosion cracking. Crack velocity $V$ is shown as a function of Mode I stress-intensity factor $K_I$. $K_{IC}$ is the critical value of $K_I$ for rapid fracture and $K_0$ is the possible threshold value below which no crack growth occurs.

II the speed of crack growth is limited by the rate at which the corrosive species can move to the crack-tip. In region III, crack growth is rapid and independent of environmental effects. The limiting value of the stress intensity factor for rapid growth is $K_{IC}$ but whether there exists a threshold value $K_0$ below which no propagation occurs is unknown.

Atkinson (1979b, 1980) has studied slow crack growth (region I) in several rocks for the range of speeds from roughly $10^{-10}$ m s$^{-1}$ to $10^{-3}$ m s$^{-1}$ and he has found the crack speeds were proportional to $K_I^n$. For quartz crystals, $n = 12$ or 20 depending on orientation; for Arkansas novaculite, a fine-grained quartz rock, $n = 25$; and for a gabbro, $n = 32$. For Westerly granite, Atkinson & Rawlings (1979a,b) found $n = 39$ for deformation in air at 30% relative humidity and $n = 34$ in liquid water (in both cases at 20°C). [Swanson & Spetzler (1979) have also reported some preliminary results for environmentally assisted crack growth in Westerly granite for crack velocities ranging from approximately $10^{-7}$ m s$^{-1}$ to 10 m s$^{-1}$.] In all cases the crack velocity at a given stress intensity factor increased with relative humidity and with temperature. The existence of a stress corrosion limit of $K_0 \simeq 0.52\, K_{IC}$ was inferred for the quartz, but no limit was observed for either the novaculite at crack velocities down to $10^{-10}$ m s$^{-1}$ (corresponding to $K = 0.6\, K_{IC}$) or for the gabbro at crack velocities down to approximately $10^{-9}$ m s$^{-1}$ (corresponding to $K \simeq 0.5\, K_{IC}$). For the novaculite, region I extended to $K_I = 0.94\, K_{IC}$ at 20°C so that regions II and III of Figure 4 may not be present.

Rice (1979b) has discussed the importance of these studies as an ingredient in more complete constitutive descriptions of the macroscopic time-dependent behavior of brittle rock and, as an example, he interprets the following observation of Wawersik & Brace (1971): when the stress on an axisymmetric compression sample of Westerly granite was held constant at a value slightly below peak stress (as determined by a test at a strain rate of about $10^{-5}$ s$^{-1}$), the sample deformed at constant stress, "tunnelled" through the peak of the stress-strain curve, and rejoined the post-peak curve. Rice (1979b) rationalized this behavior as caused by an increase in the microcrack density owing to slow crack growth at local values of the stress intensity factors which are below the levels for rapid growth. A rapid increase of stress at essentially constant microcrack density then brought the stress intensities to levels appropriate for rapid growth as the post-peak curve was rejoined. As a further example, Atkinson (1980) has used his $V$ vs $K_I$ data to predict the reduction of tensile fracture stress for Arkansas novaculite, as determined by bend experiments, from 72 MPa at a strain rate of $6 \times 10^{-5}$ s$^{-1}$ to 39 MPa at $10^{-10}$ s$^{-1}$. In addition, he suggests that his results support the contention of Rutter & Mainprice (1978) that stable sliding of wet pre-faulted Tennessee sandstone may,

under certain conditions, be controlled by environmentally assisted cracking of near-fault grains. Dieterich & Conrad (1978) have also reported some observations which suggest that the time dependence of friction (Dieterich 1972, 1978) may, at least in part, be due to environmental effects. More specifically, the presence of a humid environment both increases the rate of growth of asperity contacts and decreases the shear strength of the contacts.

Because of the slow rate of tectonic loading and the typically long recurrence intervals for earthquakes, at least by comparison to laboratory time scales, time-dependent crack growth may be important in determining long term strength levels for crustal faulting. Crack speeds of $10^{-9}$ m s$^{-1}$ may be very slow on laboratory time scales but this corresponds to 3 cm yr$^{-1}$ which is comparable to observed rates of relative slip on the San Andreas fault in central California (Savage & Burford 1973).

A recent analysis by Rice (1978a), which takes proper account of thermodynamic restrictions on the brittle growth of cracks, seems to offer a promising theoretical framework for the study of environmental effects in crack growth. He finds that thermodynamic considerations require crack growth to be compatible with the inequality

$$(G-2\Gamma_0)V > 0 \tag{25}$$

where $V$ is the crack speed (positive for extension) and the quantity in parenthesis is the difference between the energy release rate and the energy required to create new crack surface. This difference is the "force" which is thermodynamically conjugate to $V$. The condition (25) includes the Griffith criterion $G = 2\Gamma_0$ when $V = 0^+$, but Rice (1978a) has discussed the role of environmental effects in altering $\Gamma_0$. An important implication of (25) for earth faulting is that crack healing is not prohibited; that is $V$ may be negative when $G < 2\Gamma_0$. Because all models of earthquake instability, at least those consistent with the principles of mechanics, require strength loss upon faulting [see Stuart (1979) for a review], the observation of repeated earthquakes in the same location indicates that some mechanism of strength recovery is necessary. As noted by Rice (1978a) the small stress drops (10–100 bars = 1–10 MPa) in earthquakes and the extremely brittle nature of cracking on the microscale in rock make crack healing an attractive possibility. Although apparent healing of microcracks has been observed by use of a scanning electron microscope in studies of microcrack growth in rock (e.g. Kranz 1979a), to the author's knowledge no systematic study of microcrack healing has been carried out.

## *Shear Fracture and Friction Experiments*

Most seismic faulting in the earth's crust is thought to involve processes of shear fracture and frictional sliding rather than tensile fracture, although, as mentioned earlier, tensile fractures may play an important role in the formation of a macroscopic throughgoing fault. In the laboratory, however, shear fractures are unstable in the sense that they tend to propagate out of their original plane [e.g. Brace & Bombolakis (1963) and Ingraffea et al (1977); Cotterell & Rice (1979), in a reexamination of the solution for a slightly kinked crack, have shown that out-of-plane propagation occurs when the traction parallel to the crack-line is compressive]. Consequently, there are no measurements of critical values of $K$, $G$, or $J$ for shear fracture analogous to those for mode I loading. On the other hand, there have been numerous laboratory investigations of frictional sliding [see Evernden (1977) for recent work relevant to earth faulting]. Although these experiments are frequently interpreted as analogues of crustal shear faulting, Rice (1979b) has used the PR model, which was discussed earlier, to point out that the possibility for laboratory friction experiments to simulate field conditions is critically dependent on the size of the breakdown zone, that is, the distance behind the fault-tip over which the fault surface stress exceeds the residual friction level. In order for laboratory friction experiments to be geometrically similar to slip zones in the field, the breakdown zone must be small by comparison to the length of the slipping zone.

For the PR model with a small end zone and a linear decrease of stress in the end zone, the size of the end zone is obtained by multiplying Equation (23), which is for constant end zone stress, by 9/4:

$$R = (9/16)\pi\mu\delta'[(\tau_p - \tau_f)(1-\nu)]^{-1}. \tag{26}$$

The quantity $\delta'$, which is defined by Equation (21), is a measure of the slip necessary to reduce the stress in the end zone from the peak value $\tau_p$ to the residual level $\tau_f$. If $\mu = 2 \times 10^4$ MPa, $\nu = 0.3$, and $\tau_p - \tau_f$ is taken to be the same order as a representative stress drop (10 MPa), then $R = (4.42 \times 10^3)\delta'$. Rice (1979b) has inferred values of $\delta' = 2.5$ mm from data of Coulson (1972) (as quoted by Barton 1973) on a natural joint in coarse-grained granite and $\delta' = 2.5\ \mu$m from Dieterich's (1979) sliding experiments on flat ground specimens of granite. These yield $R = 1$ m and 11 mm, respectively. Rudnicki (1979), however, has suggested, based on observations of Barton (1971), that larger values of $\delta'$, for instance, on the order of centimeters, may be more representative of in situ conditions. If $\delta' = 2.5$ cm, $R = 110$ m. Barton (1971) has suggested that $\delta'$ may increase with the

length of the sliding surface. In model studies designed to simulate test specimens of different sizes, he found that peak and residual strengths for rough joints were reached after a displacement of about 1 % and 10 % of the test length, respectively. If this result can be extrapolated to faults in situ, the corresponding size of the end zone will be enormous. However, this increase presumably reflects the presence of larger wavelength surface irregularities on larger sliding surfaces which may not exist on a fault surface that has undergone a large amount of relative slip. In contrast, the resistance to sliding in Dieterich's (1979) experiments on flat ground samples is apparently due to adhesion at asperity contacts rather than to sliding over geometric irregularities.

Obviously $\delta'$ depends strongly on conditions at the surface: the nature of asperity contacts; grain size; pore pressure; whether deformation at asperity contacts occurs by brittle cracking, plastic flow, or, at elevated temperatures, by local melting and pressure solution; whether gouge or moisture is present. Despite the evident importance of this size effect in extrapolating friction experiments to in situ conditions, there have been relatively few investigations of the precise variation of frictional stress for small values of the relative offset. If the values cited for $\delta'$ are indeed representative, geometric similarity will necessitate large laboratory specimens and/or preparation of the sliding surface to produce small values of $\delta'$, as in the experiments of Dieterich (1979).

## CRITICAL ENERGY RELEASE RATES FOR CRUSTAL FAULTING

Although, as mentioned in the last section, shear fractures in the laboratory tend to propagate out of their original plane, many crustal earthquakes obviously do propagate in a way that can be idealized as a shear crack. Strong kinematic constraints or the effects of pre-existing zones of weakness may be responsible for preventing out-of-plane propagation of shear fractures on this size scale. In any case, this section reviews and discusses some estimates of the critical energy release rate for crustal faulting. Also, the critical energy release rate at the onset of the 1857 California earthquake is estimated by using the $J$ integral, current geodetic data, and Sieh's (1978a) estimate of the recurrence time for such earthquakes.

Husseini et al (1975) have estimated $G_{crit}$ corresponding to the arrest of seismic faulting. They inferred values of $1–10^4$ J m$^{-2}$ associated with frictional sliding and values of $10^4–10^6$ J m$^{-2}$ associated with fresh fracture. Ida (1973b) estimated a value of $10^7$ J m$^{-2}$ based on maximum values of ground surface displacements and acceleration. Aki (1978) has estimated

$G_{crit} = 8 \times 10^5$ J m$^{-2}$ corresponding to arrest of the 1966 Parkfield earthquake and $G_{crit} = 10^8$ J m$^{-2}$ associated with fracture barriers during the 1857 California earthquake. Rice & Simons (1976) obtained $G_{crit} = 2.6 \times 10^2$ J m$^{-2}$ from observations by King, Nason & Tocher (1973) of a creep event on the San Andreas fault. Of these estimates, the last is likely to be the most accurate because, as Rice & Simons note, the observed displacement profile for the creep event was very nearly elliptical in agreement with the prediction of Equation (10) for the relative surface displacements of a fault with constant stress applied to the fault surfaces and no net enclosed dislocation. However, because this estimate was for a creep event the value of $G_{crit}$ is probably lower than that for a typical seismic rupture.

The estimates of Aki (1978) tend to be higher than the others because they are based on an interpretation of faulting in terms of the "barrier" model introduced by Das & Aki (1977b). As mentioned earlier, the discretization of the fracture criteria in this work introduces a characteristic length whose physical significance has not yet been established. Aki (1978), however, actually estimates $G_{crit}$ based on the dynamic version of Equation (11) (see Freund 1976a,b, 1979) for the propagation of a fault with a sharp tip. For comparison Husseini et al (1975) estimated $G_{crit} = 1.1 \times 10^2$ J m$^{-2}$ for arrest of the Parkfield earthquake, a value 7000 times smaller than that obtained by Aki (1978) for the same event. The difference occurs because Aki (1978) used a stress drop (5 MPa) inferred from accelerogram data, which presumably reflects a local value, and an effective fault length of 3 km corresponding to a "barrier interval" inferred from the aftershock data, whereas the fault length inferred from the surface rupture was 35 km.

An application of the $J$ integral to the idealized geometry in Figure 5 can be used to estimate $G_{crit}$ for initiation of the 1857 California earthquake. Figure 5 is meant to idealize a long strike-slip fault which is locked to the right of point $T$, but which is undergoing steady relative displace-

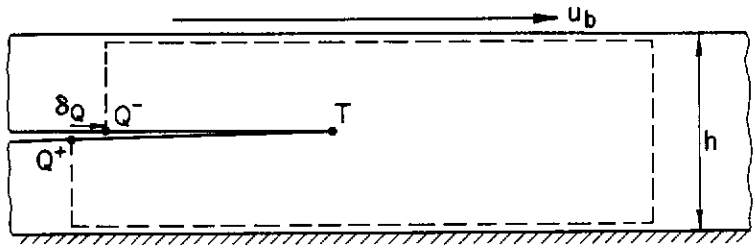


*Figure 5* Idealization of a long strike-slip fault loaded by displacements $u_b$. Relative slip at point $Q$ is $\delta_Q$.

ment to the left of $T$. At point $Q$ the relative displacement is $\delta_Q$. The fault is loaded by displacements $u_b$ at a distance $h/2$ from the fault. These displacements are assumed to be imposed by the large scale relative plate motion. Calculation of the $J$ integral [Equation (13)] for the contour shown in Figure 5 follows exactly the calculation of PR for a long shear box apparatus and, consequently, details are omitted. It is, however, clear that only the vertical end segments contribute to the integral because of the imposed displacements on the top and bottom. Path independence of $J$ requires that the value for this contour be equal to that for a contour along the fault surfaces (with the same endpoints). The result is [from Equation (17) of PR, after using their (16)]

$$J_Q - \tau_f \delta_Q = (h/2)\mu(\gamma^+ - \gamma^-)^2 \tag{27}$$

where $\gamma^+ = u_b/h$ is the uniform strain well ahead of point $T$ and $\gamma^- = \gamma^+ - \delta_Q/h$ is the uniform strain in the material adjacent to the fault near point $Q$. Use of the expression for $\gamma^-$ in (27) yields

$$J_Q - \tau_f \delta_Q = \mu \delta_Q^2/(2h) \tag{28}$$

where, from Equation (20) and Equation (21), the left-hand side is equal to the work necessary to overcome the cohesive forces and advance the fracture. For a small end zone, this work is equal to the energy release rate.

The San Andreas fault is approximately straight in central California and Figure 5 is a reasonable idealization of the deformation pattern. The fault tip (point $T$) is in the vicinity of Cholame. To the northeast (left in Figure 5), the fault is creeping and to the southwest the fault is locked, although in the area of Parkfield-Cholame, both creep and seismic faulting are intermittently observed (Sieh 1978b). The observed relative displacement rate on the creeping portion is about 3 cm/year (Savage & Burford 1973). Thatcher (1979) has discussed geodetic measurements from a net which has a width of 60 km and includes the fault. The relative displacement rate measured across the net indicates right lateral plate motion of 3.3 to 4.5 cm/year in the last 100 years. Although this is less than the 5.6 cm/year obtained by Minster & Jordan (1978) from the kinematics of global plate motions, taking $h = 60$ km would seem to be a reasonable estimate of the distance at which the motion is effectively imposed by displacements. Sieh (1978a) has estimated an average recurrence time of 160 years for 1857-type earthquakes, and thus, $\delta_Q = (160\ \text{yr}) \times (3\ \text{cm/yr}) = 480$ cm. Substituting this value, $\mu = 2 \times 10^4$ MPa and $h = 60$ km into (28) yields

$$J_Q - \tau_f \delta_Q = G_{\text{crit}} = 3.8 \times 10^6\ \text{J m}^{-2}. \tag{29}$$

This calculation must, of course, be regarded as an order of magnitude estimate but it would seem to be at least as accurate as the other estimates of $G_{crit}$ except for that of Rice & Simons (1976). It should also be emphasized that the calculation pertains to the onset of rupture whereas a much smaller value of $G$ may be necessary to continue rupture. A model with more detailed assumptions about the distribution of fault surface stress near the end of the fault might provide a mechanical basis for the foreshock sequence which Sieh (1978b) suggests is characteristic of these earthquakes.

The range of values for $G_{crit}$ which have been estimated from field observations is so large and the estimates are, in general, so rough that it is difficult to know what significance should be attached to them. Some perspective may be obtained by comparison of these values with those corresponding to laboratory tensile fracture (although there is no evident reason why these values should be related) and with estimates of seismic energy radiated in earthquakes. The smallest values of $G_{crit}$ obtained by Husseini et al (1975) for frictional sliding ($1–10^2$ J m$^{-2}$) and the value obtained by Rice & Simons (1976) for fault creep are comparable in magnitude to those obtained in laboratory tests on tensile fracture. More generally, however, the values estimated from field observations are much greater than those obtained from laboratory measurements. Nevertheless, even the largest values of $G_{crit}$, when multiplied by the fault area, yield an energy much less than empirical estimates of the seismic energy released by earthquakes. For example, the 1857 California earthquake had a rupture length of about 275 km (Sieh 1978a) and if it is assumed that the rupture extended to 10-km depth, the fracture energy is about $10^{15}$ J for $G_{crit} \simeq 10^6$ J m$^{-2}$. Use of Sieh's (1978a) estimate of the surface wave magnitude for this earthquake $M_S = 8.25$ in the Gutenberg-Richter relationship [p. 366 of Richter (1958) with correction noted by Kanamori & Anderson (1975)]

$$\log E = 11.8 + 1.5\, M_S \qquad (30)$$

yields a value for the seismic energy of $10^{21}$ J. For smaller earthquakes, the fracture energy may be more comparable to the total seismic energy. For $M_S = 6.0$ Equation (30) yields $E \simeq 10^{17}$ J. The data plotted in Figure 5 of Kanamori & Anderson (1975) suggest a fault area of about 100 km$^2$ for $M_S = 6.0$ and, if $G_{crit} = 10^6$ J m$^{-2}$, the corresponding fracture energy is $10^{15}$ J.

It is, of course, important to remember that such estimates reflect values that are averaged over the fault plane and the critical value of the energy release rate needed to extend the fault is likely to be extremely nonuniform. More specifically, $G_{crit}$ is likely to be very high where

"asperities" lock the fault and low where the resistive stress is at the residual friction level. The higher values of $G_{crit}$, which were estimated by Aki(1978), may correspond to the values at asperities. Although the present estimates of $G_{crit}$ are of limited usefulness, the study of the critical energy release rate would seem to be a worthwhile approach to obtaining more detailed information about the earthquake rupture process in general, and the nature of nonuniform rupture in particular. There has been a large amount of empirical data accumulated on earthquakes that seems to be consistent with simple physical models (e.g. Kanamori & Anderson 1975). It would be useful to investigate the possibility of similar relationships involving $G_{crit}$. For example, if, as suggested above, the fracture energy is a larger proportion of the seismic energy for smaller earthquakes, it is unlikely that small earthquakes could be considered "similar" to larger events.

## TIME-DEPENDENT EFFECTS IN FAULTING

Although earth faulting is typically a very brittle event, observations of fault creep (Goulty et al 1978), slow precursors (Kanamori & Cipar 1974), tsunami earthquakes (Fukao 1979), slow earthquakes (Sacks et al 1977), and migration of aftershocks (Melosh 1976) all suggest that deviations from purely brittle behavior are frequent. Moreover, because observations of very slow faulting events that do not generate extensive seismic waves are limited to areas well-instrumented with creep or strain meters, such events may be more prevalent than present observations suggest. Time-dependent effects may arise from a number of sources: stress corrosion cracking, plastic creep, or coupling of the deformation with diffusion of an infiltrating pore fluid are examples. Moreover, for very large earthquakes, the coupling between the asthenosphere and the lithosphere will introduce time-dependent effects into the response. In this section, some results for the spreading of shear faults in viscoelastic and fluid-infiltrated porous elastic solids will be reviewed. In addition to their relevance to the geophysical phenomena noted above, these examples will illustrate the fundamental inadequacy of the Griffith fracture criterion when applied to nonelastic solids.

In the earlier discussion of fracture criteria, it was emphasized that the cohesive force model was equivalent to the Griffith approach if the end zone size was small and the material was elastic. The Griffith approach is convenient in that the actual microstructural processes of fracture that occur in the breakdown zone can be ignored in favor of regarding the crack-tip as a singularity in the elastic stress field. Energy changes of the

body can then be calculated from the singular elastic field and the microstructural processes of breakdown enter only in defining a critical value of the energy release rate (or, equivalently, a critical value of $K$, $J$, or any other parameter characterizing the deformation near the crack-tip, since these are all related for a small end zone) at which fracture occurs. Rice (1966), however, drew attention to some difficulties with application of the Griffith approach to fracture in nonelastic solids and Rice (1979a) has emphasized that all attempts to employ an energy balance of the Griffith type in nonelastic materials have led to physically unacceptable results. As Rice (1979a) explains, the difficulty is not, of course, with the notion that energy should balance, but rather with the assumption, which is implicit in the Griffith criteria, that energy changes due to crack advance can be calculated independently of the microstructural processes of breakdown. This issue has been discussed in detail by Rice (1979a) for a number of material models, but for the time-dependent materials discussed here, the effect is straightforward. The material response introduces a characteristic time, say $t^*$, which is associated with the breakdown processes. If the fault is spreading at speed $V$, then the cohesive force model will be equivalent to the Griffith model only if the size of the breakdown zone is small by comparison to $Vt^*$. This is generally not the case.

In both of the examples reviewed here attention will be restricted to steady state propagation of a mode II shear fault. The fault will be taken as semi-infinite with the loading applied over a portion of the fault surface in order to reflect, as discussed earlier, the finite length of the actual fault. Because of the anticipated inadequacy of the Griffith energy balance model, the PR cohesive zone model is employed at the outset. The Griffith model of a singular crack-tip will be recovered as a special case.

### *Viscoelastic Effects in Fault Propagation*

A number of authors (e.g. Kostrov & Nikitin 1970, Barenblatt, Entov & Salganik 1970, Mueller & Knauss 1971, Knauss 1974, Schapery 1975) have examined fracture in viscoelastic solids, but the treatment here follows Rice's (1979a) synopsis of his earlier analysis (unpublished lecture notes for graduate course in Fracture Mechanics at Brown University, Providence, R. I., 1973). For steady state fault propagation, the results can be obtained directly from the linear elastic results by means of the correspondence principle of linear viscoelasticity (Fung 1965, Knauss 1974). For the PR model with constant end zone stress, the linear elastic result for the slip in the end zone is given by (17) with $f(\lambda)$ as in (18). If the viscoelastic solid is characterized by a compliance $M(t)$ appropriate to tensile stress application to a body constrained to respond

in plane strain, then the relative slip at the end of the breakdown zone is

$$\delta(x = -R) = [K^2/(\tau_p - \tau_f)] \int_0^1 M[(1-\xi)R/V] f'(\xi)\, d\xi \tag{31}$$

where $V$ is the propagation velocity and $R$ is still given by (15). Evidently, if the short-time response of the viscoelastic solid is elastic, comparison with Equation (17) reveals that $M(0) = (1-\nu_0)/2\mu_0$ where $\nu_0$ and $\mu_0$ are the appropriate Poisson's ratio and shear modulus. Similarly, if the limiting long-time response is also elastic, $M(\infty) = (1-\nu_\infty)/2\mu_\infty$. The fracture criterion (19) can now be applied to Equation (31) where it is assumed that $\delta^*$ is independent of time. The result is

$$K^2 \int_0^1 M[(1-\xi)R/V] f'(\xi)\, d\xi = G_{crit} \tag{32}$$

where Equation (22) has been used with $\delta^* = \delta'$ for constant end zone stress. The limiting result for very slow fault propagation ($V = 0^+$) is easily extracted from (32):

$$K^2 M(\infty) = G_{crit}. \tag{33}$$

This relation defines a threshold value of the stress intensity factor $K_s = [G_{crit}/M(\infty)]^{1/2}$ below which no fault propagation is possible. For very fast propagation ($V = \infty$), (32) reduces to the expression

$$K^2 M(0) = G_{crit} \tag{34}$$

and $K_f = [G_{crit}/M(0)]^{1/2}$ defines the limiting stress intensity factor for dynamic propagation. For intermediate values of $K$, fault propagation occurs at the velocity for which (32) is satisfied, as illustrated schematically in Figure 6.

The predictions of the Griffith energy balance model can be recovered in the limit of vanishing end zone size. Letting $R \to 0$ in (32) yields Equation (34) independently of the velocity of propagation. Because $G_{crit}$

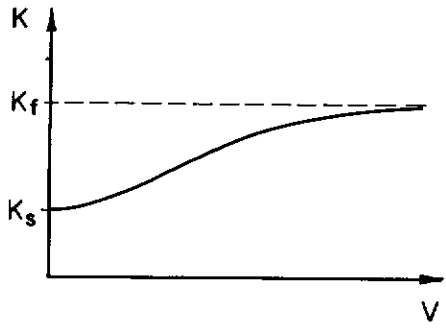


*Figure 6* Applied stress intensity factor $K$ vs fault propagation velocity $V$ for a linear viscoelastic solid. $K_f$ and $K_s$ are the critical values for fast ($V \to \infty$) and slow ($V = 0^+$) propagation, respectively.

is assumed to be a fixed material parameter, the limit $R \to 0$ corresponds to simultaneously letting $\tau_p - \tau_f \to \infty$ so that the shaded area in Figure 3*b* is constant. As mentioned earlier, the limit $R \to 0$ is appropriate only when $R \ll Vt^*$ where $t^*$ is a characteristic time for the response of the end zone material.

Although this model is very simple, its relevance to the geophysical phenomena mentioned earlier is clear. For applied loads that induce a stress intensity factor $K < K_s$, no fault propagation occurs, whereas for $K \simeq K_f$, dynamic (seismic) faulting is predicted. However, for $K_s < K < K_f$ fault growth is quasi-static. Furthermore, in this range of $K$ values, fault propagation is stable in the sense that increases in $K$ (which may result from either increases in the magnitude of the applied loads or an increase in the length of fault surface that is loaded) are necessary to increase the velocity.

The example can be carried further by assuming a specific form for $M(t)$. If the viscoelastic response is, for simplicity, assumed to be described by a linear Maxwell model, then

$$M(t) = M_0(1 + t/t_m) \tag{35}$$

where $M_0 = M(0)$ and $t_m$ is the Maxwell relaxation time. The Maxwell time can be expressed as $\eta/M_0$ where $\eta$ is a viscosity. For a Maxwell solid $M(\infty)$ is unbounded so that the threshold $K$ value for slow fault growth is zero. Although it is often stated that for $t \gg t_m$ a Maxwell solid "behaves like a viscous fluid," the imprecision of this statement when acute geometries are present is evident. In contrast to the behavior of a viscous fluid in which no crack growth would be expected, growth of any finite size crack will occur in a Maxwell solid (although it may be very slow) at any level of the applied load. Substituting (35) into (32) and performing the integration yields

$$K^2 M_0[1 + R/(3Vt_m)] = G_{crit}. \tag{36}$$

This equation can be rearranged to yield the following expression for the velocity after using (16) for $R$ and the definition of $K_f$:

$$V = (l/3t_m)[(\tau_\infty - \tau_f)/(\tau_p - \tau_f)]^2 [(K_f/K)^2 - 1]^{-1}. \tag{37}$$

Unfortunately, good estimates for the parameters in this equation are not available. If, however, $K = 0.9K_f$, $t_m = 5$ yr, $l = 100$ km, and the first term in square brackets is unity, then Equation (37) yields $V = 60$ km/yr. This velocity is typical of observed rates for migration of seismic activity along large transform fault systems (Savage 1971). For predominantly "brittle" behavior and low stress drops $K$ and $(\tau_\infty - \tau_f)$ may differ only slightly from $K_f$ and $(\tau_p - \tau_f)$, respectively. A length of 100 km seems to

be an appropriate size scale for phenomena associated with large earthquakes. A Maxwell time of five years corresponds to a shear modulus of $6 \times 10^4$ MPa and a viscosity of $10^{19}$ Poise, values that may be representative of the earth's mantle. There is, of course, disagreement about appropriate values for the viscosity of the mantle and, moreover, whether a linearly viscous model is adequate (Melosh 1976, 1978, Savage & Prescott 1978). If viscosity does vary nonlinearly with stress, the high stress near the fault tip would presumably result in a lower effective viscosity and shorter Maxwell times. In addition, laboratory tests on rock yield values ranging down to $10^{13}$ Poise (e.g. Handin 1966) so that shorter Maxwell times may be appropriate for faulting in the crust. In any case, Equation (37) illustrates the type of behavior that might be expected.

## *Coupled Deformation-Diffusion Effects in Fault Propagation*

Fluid infiltration of a porous elastic solid introduces a time dependence into the response because the deformation of the solid is coupled to the diffusion of the infiltrating pore fluid. Rice & Simons (1976; also, see Simons 1977) investigated the steady-state propagation of a plane strain (mode II) shear fault in such a fluid-infiltrated solid. The presence of diffusion introduces a length scale $c/V$ where $c$ is the diffusivity and $V$ is the propagation speed. Different regimes of behavior are obtained depending on the relative magnitudes of $c/V$, the end zone size, and the fault length. Rice & Simons demonstrated that fault propagation was stabilized by coupled deformation diffusion effects for a range of velocities, which is consistent with the range of observed creep events on the San Andreas fault. Ruina (1978) has analyzed the corresponding problem of a tensile (mode I) crack and has discussed the implications of his results for the retardation of hydraulic fractures. A complementary stabilizing effect due to coupling of pore fluid diffusion with dilatancy in the end zone has been treated by Rice (1979b; also see Rice & Cleary 1976) but will not be discussed here.

The equations governing the response of a linear fluid-infiltrated porous elastic solid were established by Biot (1941) but Rice & Cleary (1976) recently achieved a propitious rearrangement of them. For plane strain conditions (deformation is independent of $z$; $i,j = x,y$ in the following equations), the strain of the solid matrix $\varepsilon_{ij}$ and the fluid mass content per unit volume of porous medium $m$ are related to the total stress $\sigma_{ij}$ and the alteration of pore fluid pressure $p$ (from some ambient value) by

$$2\mu\varepsilon_{ij} = \sigma_{ij} - \nu(\sigma_{xx}+\sigma_{yy})\delta_{ij} + 3\{(\nu_u - \nu)/[B(1+\nu_u)]\}\delta_{ij}p \tag{38}$$

$$m-m_0 = \{3\rho_0(\nu_u-\nu)/[2\mu B(1+\nu)(1+\nu_u)]\}\cdot[(1+\nu_u)(\sigma_{xx}+\sigma_{yy})+(3/B)p] \tag{39}$$

where $m_0$ is the value of $m$ in the unstressed state and $\rho_0$ is the density of the pore fluid. The material parameters in these equations are best explained by considering the limiting cases of deformation that is very rapid and very slow by comparison to the time scale of pore fluid diffusion. In the latter case, which is said to be "drained," the deformation is slow enough so that alterations in pore fluid pressure can be alleviated by diffusive mass flux and, consequently, the pore fluid pressure is constant in time. Examination of (38) for $p = 0$ then reveals that the response is that of an ordinary linear elastic solid with $\mu$ and $\nu$ as the shear modulus and Poisson's ratio. In the alternative short-time limit, which is said to be "undrained," the deformation is too rapid to allow time for fluid mass to diffuse out of material elements. Thus, $m = m_0$ and $B$ can be identified from (39) as the ratio of the pore fluid pressure induced by undrained response to the mean normal stress. Substitution of this value for $p$ into (38) discloses that the undrained response is also that of a linear elastic solid, but with Poisson's ratio $\nu_u$ (where the subscript u denotes "undrained") rather than $\nu$. Because $\nu \leqq \nu_u \leqq 1/2$ (Rice & Cleary 1976), the response of the fluid-infiltrated solid is elastically stiffer for undrained conditions than for drained conditions and this increased stiffness is the source of the stabilizing effect in fault propagation. One additional constitutive equation is needed to describe the fluid mass flux. This is Darcy's law

$$q_i = -\rho_0\kappa\,\partial p/\partial x_i \tag{40}$$

where $q_i$ is the mass flow rate in the $x_i$ direction per unit area and $\kappa$ is a permeability.

The formulation is completed by the set of field equations that express stress equilibrium, strain compatibility, and fluid mass conservation. The equilibrium equation is

$$\partial\sigma_{ij}/\partial x_i = 0. \tag{41}$$

The conditions of strain compatibility and mass conservation yield, after some rearrangement, the following two equations:

$$\nabla^2(\sigma_{xx}+\sigma_{yy}+2\eta p) = 0 \tag{42}$$

where $\eta = 3(\nu_u-\nu)/2B(1+\nu_u)(1-\nu)$ and

$$(c\nabla^2-\partial/\partial t)[\sigma_{xx}+\sigma_{yy}+(2\eta/\xi)p] = 0 \tag{43}$$

where $\xi = (\nu_u - \nu)/(1-\nu)$ and the diffusivity is

$$c = \frac{2\mu\kappa B^2(1-\nu)(1+\nu_u)^2}{9(1-\nu_u)(\nu_u-\nu)}. \tag{44}$$

Rice & Simons (1976) first solved these equations for the case of a steadily propagating fault (at a speed $V$) with no end zone. The fault was assumed to be semi-infinite and loaded by stresses $\tau_\infty - \tau_f$ over a length $l$ of its surfaces, as in Figure 1*b*. For this geometry, the stress intensity factor for an elastic solid is given by (4). Because no material constants enter this expression, one might anticipate that the stress intensity factor for the fault in the fluid-infiltrated solid would also be given by (4) (as was the case for the linear viscoelastic solid discussed in the last section). The solution of Rice & Simons demonstrates, however, that the stress intensity factor is given by

$$K = K_{nom} h(Vl/c) \tag{45}$$

where $K_{nom}$ is given by (4) and the function $h$ decreases monotonically from unity at $Vl/c = 0$ to $\beta^{-1} = (1-\nu_u)/(1-\nu)$ as $Vl/c \to \infty$. (Because $\nu < \nu_u < 1/2$, $\beta^{-1} < 1$.) Thus $K_{nom}$ is the value of the stress intensity factor that would be caused by the applied loads in the absence of pore fluid effects. For fault propagation in a fluid-infiltrated solid, this value is attained only for zero propagation speed and the stress intensity factor for any nonzero speed is less than $K_{nom}$. Rice & Simons (1976) rationalized this result by pointing out that for a fault without an end zone, a region near the fault-tip responds in drained fashion for any finite propagation speed whereas the surrounding material further from the fault responds in undrained fashion and, consequently, is elastically stiffer. Because the region near the fault-tip is drained, the energy release rate corresponding to (45) can be calculated from Equation (11) using the drained value of Poisson's ratio. The result is

$$G = G_{nom} h^2(Vl/c) \tag{46}$$

where

$$G_{nom} = (1-\nu)K_{nom}^2/2\mu \tag{47}$$

is the energy release rate for the same applied loads but in the absence of coupled deformation diffusion effects.

If fault growth is assumed to occur when $G$ attains some critical value, say $G_{crit}$ (where $G_{crit}$ may be defined by (22) from a more detailed model of the fault-tip), then the fracture criterion is

$$G_{nom} h^2(Vl/c) = G_{crit} \tag{48}$$

This relation is shown schematically in Figure 7 by the curve labeled

$R/l = 0$ corresponding to the idealization of a vanishingly small end zone. $G_{nom}$ can be interpreted as the "driving force" supplied by the applied loads. In the absence of porous media effects the driving force would be sufficient to cause dynamic ($V \to \infty$), that is, seismic fault propagation when

$$G_{nom} = G_{crit}. \tag{49}$$

The coupling of deformation with the diffusion is, however, a stabilizing effect and dynamic fault propagation is predicted for the fluid-infiltrated solid only when the driving force rises to

$$G_{nom} = \beta^2 G_{crit}. \tag{50}$$

Moreover, fault propagation is stable in the sense that an increase in driving force ($G_{nom}$) is necessary to increase the speed of propagation. This result is, however, mitigated by the inclusion of a small, but finite size end zone.

Rice & Simons reanalyzed the problem for an end zone of length $R$ and a constant value of the end zone stress (see Figure 3). In this case, the results differ dramatically from those for a vanishingly small end zone. As shown in Figure 7, fault propagation is stable only for a range of values for $Vl/c$. The results of Equations (48–50) are recovered from the analysis for a finite size end zone in the limit $VR/c = 0$, but for nonzero $VR/c$ there are two additional limiting cases of interest. If $Vl/c \to \infty$, but

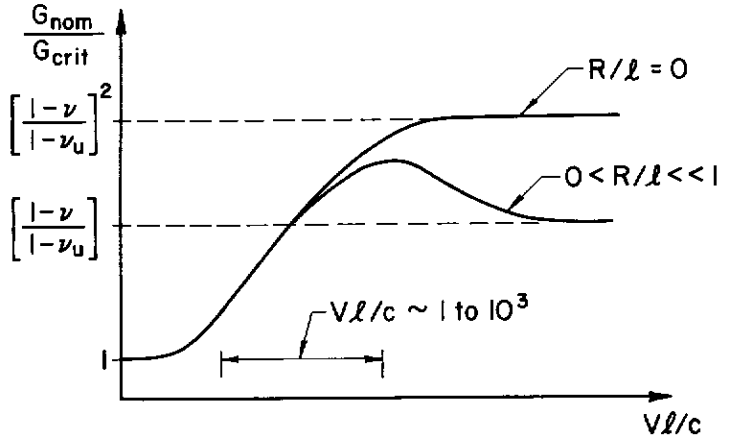


*Figure 7* After Figure 6 of Rice & Simons (1976). Nominal energy release rate as a function of fault speed $V$ for propagation in a elastic fluid-infiltrated solid with hydraulic diffusivity $c$ and Poisson's ratios $\nu$ (drained) and $\nu_u$ (undrained). Effective fault length is $l$ and end zone size is $R$. Arrow denotes range of creep events observed on the San Andreas fault by King, Nason & Tocher (1973).

$VR/c$ is finite, the response on the overall size scale is undrained but the response on the size scale of the end zone is intermediate between drained and undrained. This limit corresponds to the falling portion of the curve in Figure 7, and thus $G_{nom}$ decreases with increasing $V$. If both $VR/c$ and $Vl/c$ approach infinity with $R/l$ fixed, the response is undrained on both the overall size scale and the size scale of the end zone and

$$G_{nom} = \beta G_{crit}. \tag{51}$$

The magnitude of the stabilizing effect can be judged by the increase in driving force ($G_{nom}$) required to propagate the fault over that value ($G_{crit}$) necessary to propagate the fault in the absence of coupled deformation diffusion effects. The maximum value of $G_{nom}/G_{crit}$ lies between $\beta$ and $\beta^2$. For brittle rock, $\nu = 0.2$ and $\nu_u = 0.3$–$0.4$ are typical (Rice & Cleary 1976) and the corresponding values of $\beta$ range from 1.14–1.33. For clay soils this stabilizing effect can be even more significant as $\nu = 0.15$ and $\nu_u = 0.5$ are typical values and, thus, $\beta = 1.667$.

The existence of the falling portion of the curve in Figure 7 predicts that there is a definite range of velocities for which stable creep events are possible. If the driving force corresponding to the peak in the curve is exceeded, the fault will accelerate and propagate dynamically. From the observations of creep events by King, Nason & Tocher (1973), Rice & Simons (1976) estimate slip lengths $l$ in range 0.1–10 km and velocities $V$ in the range 1–10 km/day. Anderson & Whitcomb (1975), on the basis of a variety of field observations, have suggested a value of the diffusivity $c = 1.0\,m^2/s$ and Rice & Simons (1976) have argued that this value is reasonable for fissured rock. Rice (1979b) estimated a value of $c = 0.1\,m^2/s$ from measurements by Kovach et al (1975) of water level changes in wells. For these ranges of numerical values, the corresponding values of $Vl/c$ do indeed fall on the rising portion of the curve, as predicted by the analysis. This agreement, although suggestive, does not, of course, mean that all creep events involve stabilization by pore fluid effects. The viscoelastic effects discussed in the last section offer an alternative mechanism and a mechanism based on time-dependent friction, as observed by Dieterich (1972, 1978), is another possibility. Nevertheless, the result of Rice & Simons and its consistency with observation is an indication of the role the mechanical coupling of pore fluid diffusion with deformation can play in processes of crustal faulting. Unfortunately, the overemphasis and ensuing controversy over the possible role of pore fluid in altering seismic wave travel times has been detrimental to an appreciation of this effect. It does appear to be worthy of further study.

## PROBLEMS OUTSIDE THE REALM OF FRACTURE MECHANICS

This article has focused on the usefulness of fracture mechanics as an approach to problems of faulting and fracture of the earth's crust. In particular, the fracture criteria was emphasized as an important means for understanding the mechanical conditions that cause the onset of rupture and that distinguish different types of rupture, for example, stable creep versus seismic faulting. It would, however, be misleading to conclude the article without mentioning some difficulties with this approach and briefly reviewing some results for problems of rupture that do not fit within the present framework of fracture mechanics. There is much that is not understood about failure of the earth's crust, and, although fracture mechanics can be helpful in approaching many problems, it will not, of course, be advantageous or even possible to apply it to all problems.

The results reviewed here were, for the most part, obtained for fractures that sustained a uniform stress, except possibly in a small end zone. If the fault surface stress is very nonuniform, the situation is much more complicated and there may be difficulty in even defining a discrete end zone. Also, if the stress on the entire fault depends on the relative slip, then, in effect, the entire fault is in the breakdown zone. In this case the dislocation approach discussed earlier is advantageous and has been employed by, for example, Stuart & Mavko (1979) and Cleary (1976).

More generally, departures from elastic or linear behavior will not be confined to a narrow zone that can be idealized as a crack. Although faults are often observed to be relatively narrow features, these may be merely the final result of processes of inelastic deformation in a larger volume. Rudnicki (1977a) has suggested an inclusion model of faulting in which an ellipsoidal zone of inelastically deforming material is considered to be embedded in an infinite nominally elastic rock mass. The rock mass is loaded by far-field stresses or strains and these drive the inclusion material past peak stress and into the strain softening regime. Eventually, the inclusion material softens sufficiently that the response to an increment of far-field loading is no longer quasi-static and a dynamic (seismic) "runaway" of inclusion strain occurs. Rudnicki (1977a) derived conditions for the onset of the runaway instability in terms of the geometry of the inclusion, the moduli of the surrounding elastic material, and parameters describing the inelastic response of the inclusion material. Rice & Rudnicki (1979) used a solution of Rice, Rudnicki & Simons

(1978) for the deformation of a spherical inclusion in an elastic fluid-infiltrated solid to examine the transient stabilization of runaway instability by coupled deformation-diffusion effects.

Rudnicki (1977a) also used the results of a study by Rudnicki & Rice (1975) to determine conditions for which the deformation in the inclusion would become concentrated into a narrow zone. He found that these conditions are generally met prior to the onset of runaway instability. Although such localization of deformation may result from the growth of local inhomogeneities or the propagation of crack-like flaws, Rudnicki & Rice (1975) adopted the point of view, which was suggested by Rice (1973), that this phenomenon could be explained in terms of the constitutive description of homogeneous deformation. More specifically, conditions were sought for which the constitutive behavior allowed a bifurcation from homogeneous deformation corresponding to nonuniform deformation in a narrow band. A general review of this approach has been given by Rice (1976) and by Cleary & Rudnicki (1976) in the context of rupture in geological materials. Rudnicki (1977a,b,c) has argued that the predictions of Rudnicki & Rice (1975) are consistent with faulting of brittle rock in laboratory specimens, at least if instability is not caused by the testing machine and inhomogeneities introduced by the end constraints are minimized.

Faulting in the earth's crust seems to occur most frequently in areas where the deformation has already been localized due to some past history of faulting. Nevertheless, for earthquakes that fracture fresh or largely rehealed rock, localization of deformation may be important in processes leading up to rupture. Indeed, recent observations of the seismicity patterns prior to the San Fernando earthquake (Ishida & Kanamori 1977) are suggestive of localization of deformation. Moreover, Rice (1978b) has suggested that the difference reported by Lindh, Fuis & Mantis (1978) in the orientations for fault plane solutions of foreshocks as compared with the mainshocks is consistent in magnitude and sense with predictions of Rudnicki & Rice (1975).

## ACKNOWLEDGMENTS

Support from the Department of Theoretical and Applied Mechanics of the University of Illinois at Urbana-Champaign is gratefully acknowledged. A portion of this review was prepared while I was visiting Geophysicist at the US Geological Survey at Menlo Park, California, during June, 1979.

*Literature Cited*


Abou-Sayed, A. S. 1977. Fracture toughness $K_{IC}$ of triaxially loaded Indiana Limestone. In *Energy Resources and Excavation Technology, Proc. US Symp. Rock Mech., 18th, Keystone, Colo. 1977*, ed. F. Wang, G. B. Clark, pp. 2A3-1–2A3-8

Abou-Sayed, A. S., Brechtel, C. E., Clifton, R. J. 1978. In-situ stress determination by hydro-fracturing: a fracture mechanics approach. *J. Geophys. Res.* 83:2851–62

Aki, K. 1978. Origin of the seismic gap: what initiates and stops a rupture propagation along a plate boundary? In *Proceedings of Conference VI, Methodology for Identifying Seismic Gaps and Soon-to-Break Gaps*, convened under auspices of National Earthquake Hazards Reduction Program, 25–27 May 1978 (USGS open file report 78-943), pp. 3–46

Anderson, D. L., Whitcomb, J. H. 1975. Time-dependent seismology. *J. Geophys. Res.* 80:718–32

Anderson, O. L., Grew, P. C. 1977. Stress corrosion theory of crack propagation with applications to geophysics. *Rev. Geophys. Space Phys.* 15:77–104

Andrews, D. J. 1976a. Rupture propagation with finite stress in anti-plane strain. *J. Geophys. Res.* 81:3575–82

Andrews, D. J. 1976b. Rupture velocity of plane strain shear cracks. *J. Geophys. Res.* 81:5679–87

Atkinson, B. K. 1979a. Fracture toughness of Tennessee sandstone and Carrara marble using the double torsion testing method. *Int. J. Rock Mech. Min. Sci. Geomech. Abstr.* 16:49–53

Atkinson, B. K. 1979b. A fracture mechanics study of subcritical tensile cracking of quartz in wet environments. *Pure Appl. Geophys.* 117: In press

Atkinson, B. K. 1980. Stress corrosion and the rate dependent tensile failure of a fine-grained quartz rock. *Tectonophysics* 64: In press

Atkinson, B. K., Rawlings, R. D. 1979a. *Acoustic emission during subcritical tensile cracking of gabbro and granite.* Presented at Spring meet. Am. Geophys. Union

Atkinson, B. K., Rawlings, R. D. 1979b. Acoustic emission characteristics of subcritical and fast tensile cracking in rock. *Proc. Inst. Acoustics.* In press

Barenblatt, G. I. 1962. Mathematical theory of equilibrium cracks in brittle fracture. *Adv. Appl. Mech.* 7:55–129

Barenblatt, G. I., Entov, V. M., Salganik, R. L. 1970. Some problems of the kinetics of crack propagation. In *Inelastic Behavior of Solids, Battelle Institute Materials Science Colloquia, 4th, Columbus, Ohio, 1969*, ed. M. L. Kanninen et al., pp. 559–84. New York: McGraw-Hill. 743 pp.

Barnett, D. M., Freund, L. B. 1975. An estimate of strike-slip fault friction stress and fault depth from surface displacement data. *Bull. Seismol. Soc. Am.* 65:1259–66

Barton, N. 1971. A relationship between joint roughness and joint shear strength. *Proc. Int. Symp. Rock Mech., Nancy*, Pap. I-8

Barton, N. 1973. Review of a new strength criterion for rock joints. *Eng. Geol.* 7: 287–332

Bilby, B. A., Cottrell, A. H., Swindon, K. H. 1963. The spread of plastic yield from a notch. *Proc. R. Soc. London Ser. A* 272:304–14

Bilby, B. A., Eshelby, J. D. 1968. Dislocations and the theory of fracture. See Liebowitz 1968, 1:99–182

Biot, M. A. 1941. General theory of three-dimensional consolidation. *J. Appl. Phys.* 12:155–64

Brace, W. F. 1964. Brittle fracture of rocks. In *State of Stress in the Earth's Crust*, ed. W. R. Judd, pp. 111–74. New York: Elsevier

Brace, W. F., Bombolakis, E. G. 1963. A note on brittle crack growth in compression. *J. Geophys. Res.* 68:3709–13

Broek, D. 1974. *Elementary Engineering Fracture Mechanics.* Leyden: Noordhoff International. 408 pp.

Brown, W. F., Srawley, J. E. 1966. *Plane strain crack toughness testing of high strength metallic materials, ASTM Spec. Tech. Publ. No. 410.* Philadelphia: Am. Soc. Test. Mater. 129 pp.

Budiansky, B., Rice, J. R. 1973. Conservation laws and energy-release rates. *J. Appl. Mech.* 40:201–3

Budiansky, B., Rice, J. R. 1979. An integral equation for dynamic elastic response of an isolated 3-D crack. *Wave Motion* 1: 187–92

Cherepanov, G. P. 1968. Cracks in solids. *Int. J. Solids Struct.* 4:811–31

Cleary, M. P. 1976. Continuously distributed dislocation model for shear bands in geological materials. *Int. J. Num. Methods Eng.* 10:679–702

Cleary, M. P., Rudnicki, J. W. 1976. The initiation and propagation of dilatant rupture zones in geological materials. In *The Effect of Voids on Material Deformation*, ed. S. C. Cowin, pp. 13–30. New York: Am. Soc. Mech. Eng. Appl. Mech. Div. Vol. 16

Clifton, R. J., Simonsen, E. R., Jones, A. H., Green, S. J. 1976. Determination of critical stress intensity factor $K_{IC}$ from internally pressurized thick walled vessels. *Exp. Mech.* 16:233–38

Cotterell, B., Rice, J. R. 1979. Slightly curved or kinked cracks. *Int. J. Fract.* In press

Coulson, J. H. 1972. Shear strength of flat surfaces in rock. In *Proc. US Symp. Rock Mech., 13th, Urbana, Ill. 1971*, ed. E. J. Cording, pp. 77–105

Das, S., Aki, K. 1977a. A numerical study of two-dimensional spontaneous rupture propagation. *Geophys. J. R. Astron. Soc.* 50:643–68

Das, S., Aki, K. 1977b. Fault plane with barriers: a versatile earthquake model. *J. Geophys. Res.* 82:5658–70

Dieterich, J. H. 1972. Time-dependent friction in rocks. *J. Geophys. Res.* 77: 3690–97

Dieterich, J. H. 1978. Time-dependent friction and the mechanics of stick-slip, *J. Geophys. Res.* 116:790–806

Dieterich, J. H. 1979. Modeling of rock friction, part I: experimental results and constitutive equations. *J. Geophys. Res.* 84:2161–68

Dieterich, J. H., Conrad, G. 1978. Mechanism of unstable slip in rock friction experiments. *EOS, Trans. Am. Geophys. Union* 59:1206

Dmowska, R. 1973. Crack fault model and surface deformation associated with dip-slip faulting. *Publ. Inst. Geophys. Polish Acad. Sci.* 62:124–39

Dugdale, D. S. 1960. Yielding of steel sheets containing slits. *J. Mech. Phys. Solids* 8:100–4

Edmunds, T. M., Willis, J. R. 1976. Matched asymptotic expansions in non-linear fracture mechanics—I. Longitudinal shear of an elastic perfectly-plastic specimen. II. Longitudinal shear of an elastic work hardening plastic specimen. *J. Mech. Phys. Solids* 24:205–38

Eshelby, J. D. 1956. The continuum theory of lattice defects. In *Progress in Solid State Physics*, ed. F. Seitz, D. Turnbull. 3:79–144

Eshelby, J. D. 1970. Energy relations and the energy-momentum tensor in continuum mechanics. See Barenblatt et al 1970, pp. 77–115

Evernden, J. F., ed. 1977. *Proc. Conf. II, Experimental Studies of Rock Friction with Application to Earthquake Prediction*, convened under auspices of National Earthquake Hazards Reduction Program, 28–30 April 1977.

Freund, L. B. 1976a. Dynamic crack propagation. In *The Mechanics of Fracture*, ed. F. Erdogan, pp. 105–34. New York: Am. Soc. Mech. Eng. Appl. Mech. Div.

Freund, L. B. 1976b. The analysis of elastodynamic crack-tip stress fields. In *Mechanics Today*, ed. S. Nemat-Nasser, 3:55–91. Elmsford, NY: Pergamon

Freund, L. B. 1979. The mechanics of dynamic shear crack propagation. *J. Geophys. Res.* 84:2199–209

Freund, L. B., Barnett, D. M. 1976. A two-dimensional analysis of surface deformation due to dip slip faulting. *Bull. Seismol. Soc. Am.* 66:667–75

Fukao, Y. 1979. Tsunami earthquakes and subduction processes near deep-sea trenches. *J. Geophys. Res.* 84:2303–14

Fung, Y. C. 1965. *Foundations of Solid Mechanics*. Englewood Clifts, NJ: Prentice-Hall. 525 pp.

Goulty, N. R., Burford, R. O., Allen, C. R., Gilman, R., Johnson, C. E., Keller, R. P. 1978. Large creep events on the Imperial fault, California. *Bull. Seismol. Soc. Am.* 68:517–21

Griffith, A. A. 1920. The phenomena of rupture and flow in solids. *Philos. Trans. R. Soc. London Ser. A* 221:163–98

Handin, J. 1966. Strength and ductility. In *Handbook of Physical Constants*, ed. S. P. Clark Jr., *Geol. Soc. Am. Mem.* 97:238–89

Heaton, T. H., Helmberger, D. V. 1978. Predictability of strong ground motion in the Imperial Valley: modeling the M4.9 November 4, 1976 Brawley earthquake. *Bull. Seismol. Soc. Am.* 68:31–48

Husseini, M. I., Jovanovich, D. B., Randall, M. J., Freund, L. B. 1975. The fracture energy of earthquakes. *Geophys. J.* 43: 367–85

Ida, Y. 1972. Cohesive force across the tip of a longitudinal shear crack and Giffith's specific surface energy. *J. Geophys. Res.* 77:3796–805

Ida, Y. 1973a. Stress concentration and unsteady propagation of longitudinal shear cracks. *J. Geophys. Res.* 78:3418–29

Ida, Y. 1973b. The maximum acceleration of seismic ground motion. *Bull. Seismol. Soc. Am.* 63:959–68

Ingraffea, A. R., Heuze, F. E., Ko, H. Y., Gerstle, K. 1977. An analysis of discrete fracture propagation in rock loaded in compression. See Abou-Sayed 1977, pp. 2A4-1–2A4-7

Ishida, M., Kanamori, H. 1977. The spatio-temporal variation of seismicity before the 1971 San Fernando earthquake, California. *Geophys. Res. Lett.* 4:345–46

Jaeger, J. C., Cook, N. G. W. 1976. *Fundamentals of Rock Mechanics*. New York: Halsted. 585 pp. 2nd ed.

Kanamori, H., Anderson, D. L. 1975. Theoretical basis of some empirical relations in seismology. *Bull. Seismol. Soc. Am.* 65: 1073–95

Kanamori, H., Cipar, J. J. 1974. Focal processes of the great Chilean earthquake, May 33, 1960. *Phys. Earth Planet. Inter.* 9: 128–36

Kassir, M. K., Sih, G. C. 1966. Three-dimensional stress distribution around an elliptical crack under arbitrary loadings. *J. Appl. Mech.* 33: 601–11

King, C.-Y., Nason, R. D., Tocher, D. 1973. Kinematics of fault creep. *Philos. Trans. R. Soc. London Ser. A* 274: 355–60

Knauss, W. G. 1974. On the steady propagation of a crack in a viscoelastic sheet. In *Deformation and Fracture of High Polymers. Battelle Inst. Mater. Sci. Colloq., 7th, Kronberg im Taunus, 1972*, ed. H. H. Kausch, J. A. C. Hassell, R. I. Jaffee. New York: Plenum. 644 pp.

Knott, J. F. 1973. *Fundamentals of Fracture Mechanics*. New York: Halsted. 273 pp.

Knowles, J. K., Sternberg, E. 1972. On a class of conservation laws in linearized and finite elastostatics. *Arch. Rational Mech. Anal.* 44: 187–211

Kobayashi, T., Fourney, W. L. 1978. Experimental characterization of the development of the microcrack process zone at a crack-tip in rock under load. In *Proc. US Symp. Rock Mech., 19th, Stateline, Nev. 1978*, ed. Y. S. Kim, pp. 243–46

Kostrov, B. V., Nikitin, L. V. 1970. Some general problems of mechanics of brittle fracture. *Arch. Mech. Stosowanej* 22: 749–76

Kovach, R. L., Nur, A., Wesson, R. L., Robinson, R. 1975. Water-level fluctuations and earthquakes on the San Andreas fault zone. *Geology* 3: 437–40

Kranz, R. L. 1979a. Crack growth and development during creep of Barre granite. *Int. J. Rock Mech. Min. Sci. Geomech. Abstr.* 16: 23–35

Kranz, R. L. 1979b. Crack-crack and crack-pore interactions in stressed granite. *Int. J. Rock Mech. Min. Sci. Geomech. Abstr.* 16: 37–47

Lawn, B. R., Wilshaw, T. R. 1975. *Fracture of Brittle Solids*. New York: Cambridge Univ. Press. 204 pp.

Liebowitz, H., ed. 1968. *Fracture: An Advanced Treatise*. Volumes I-VII. New York: Academic

Lindh, A., Fuis, G., Mantis, C. 1978. Seismic amplitude measurements suggest foreshocks have different focal mechanisms than aftershocks. *Science* 201: 56–59

Martin, R. J. 1972. Time-dependent crack growth in quartz and its application to creep in rocks. *J. Geophys. Res.* 77: 1406–19

Martin, R. J., Durham, W. B. 1975. Mechanisms of crack growth in quartz. *J. Geophys. Res.* 80: 4837–44

McGarr, A., Spottiswoode, S. M., Gay, N. C., Ortlepp, W. D. 1979. Observations relevant to seismic driving stress, stress drop, and efficiency. *J. Geophys. Res.* 84: 2251–63

Melosh, H. J. 1976. Non-linear stress propagation in the earth's upper mantle. *J. Geophys. Res.* 81: 5621–32

Melosh, H. J. 1978. Reply to Savage & Prescott, 1978. *J. Geophys. Res.* 83: 5009–10

Minster, J. B., Jordan, T. H. 1978. Present-day plate motions. *J. Geophys. Res.* 83: 5331–54

Mueller, H. K., Knauss, W. G. 1971. Crack propagation in a viscoelastic sheet. *J. Appl. Mech.* 38: 483–88

Palmer, A. C., Rice, J. R. 1973. The growth of slip surfaces in the progressive failure of overconsolidated clay. *Proc. R. Soc. London Ser. A* 332: 527–48

Paris, P. C., Sih, G. C. 1965. Stress analysis of cracks. In *Fracture Toughness Testing and Its Applications, ASTM Spec. Tech. Publ. 381*, pp. 30–76. Philadelphia: Am. Soc. Test. Mater. 409 pp.

Rice, J. R. 1966. An examination of the fracture mechanics energy balance from the point of view of continuum mechanics. In *Proc. Int. Conf. Fract., 1st*, ed. T. Yokobori, 1: 283–308. Tokyo: Japanese Soc. Strength and Fracture

Rice, J. R. 1968a. Mathematical analysis in the mechanics of fracture. See Liebowitz 1968 II: 191–311

Rice, J. R. 1968b. A path independent integral and the approximate analysis of strain concentration by notches and cracks. *J. Appl. Mech.* 35: 379–86

Rice, J. R. 1973. The initiation and growth of shear bands. In *Plasticity and Soil Mechanics*, ed. A. C. Palmer, pp. 263–74. Cambridge, England: Cambridge Univ. Eng. Dept.

Rice, J. R. 1976. The localization of plastic deformation. In *Proc. Int. Cong. Theor. Appl. Mech., 14th*, ed. W. T. Koiter, 1: 207–20. Amsterdam: North-Holland

Rice, J. R. 1978a. Thermodynamics of the quasi-static growth of Griffith cracks. *J. Mech. Phys. Solids* 26: 61–78

Rice, J. R. 1978b. Models for the inception of earthquake rupture. *EOS, Trans. Am. Geophys. Union* 59: 1204

Rice, J. R. 1979a. The mechanics of quasi-static crack growth. In *Proc. US Natl. Congr. Appl. Mech., 8th, UCLA., June*

*1978*, ed. R. E. Kelly, pp. 191–216. North Hollywood, Calif: Western Periodicals
Rice, J. R. 1979b. Theory of precursory processes in the inception of earthquake rupture. *Gerlands Beitr. Geophys.* 88: 91–127
Rice, J. R., Cleary, M. P. 1976. Some basic stress diffusion solutions for fluid-saturated elastic porous media with compressible constituents. *Rev. Geophys. Space Phys.* 14:227–41
Rice, J. R., Rudnicki, J. W. 1979. Earthquake precursory effects due to pore fluid stabilization of a weakening fault zone. *J. Geophys. Res.* 84:2177–94
Rice, J. R., Rudnicki, J. W., Simons, D. A. 1978. Deformation of spherical cavities and inclusions in fluid-infiltrated elastic materials. *Int. J. Solids Struct.* 14:289–303
Rice, J. R., Simons, D. A. 1976. The stabilization of spreading shear faults by coupled deformation-diffusion effects in fluid-infiltrated porous materials. *J. Geophys. Res.* 81:5322–34
Richter, C. F. 1958. *Elementary Seismology.* San Francisco: Freeman. 768 pp.
Rudnicki, J. W. 1977a. The inception of faulting in a rock mass with a weakened zone. *J. Geophys. Res.* 82:844–54
Rudnicki, J. W. 1977b. *Localization of Deformation, Brittle Rock Failure and a Model for the Inception of Earth Faulting.* PhD thesis. Brown Univ., Providence, R.I.
Rudnicki, J. W. 1977c. The effect of stress induced anisotropy on a model of brittle rock failure as localization of deformation. See Abou-Sayed 1977, pp. 3B4-1–3B4-8
Rudnicki, J. W. 1979. The stabilization of slip on a narrow weakening fault zone by coupled deformation–pore fluid diffusion. *Bull. Seismol. Soc. Am.* 69:1011–26
Rudnicki, J. W., Rice, J. R. 1975. Conditions for the localization of deformation in pressure-sensitive dilatant materials. *J. Mech. Phys. Solids* 23:371–94
Ruina, A. 1978. Influence of coupled deformation-diffusion effects on retardation of hydraulic fracture. See Kobayashi & Fourney 1978, pp. 274–82
Rutter, E. H., Mainprice, D. H. 1978. The effect of water on stress relaxation of faulted and unfaulted sandstone. *Pure Appl. Geophys.* 116:634–54
Sacks, I. S., Suyehiro, S., Linde, A. T., Snoke, J. A. 1977. The existence of slow earthquakes and the redistribution of stress in seismically active regions. *EOS, Trans. Am. Geophys. Union* 58:437
Savage, J. C. 1971. A theory of creep waves propagating along a transform fault. *J. Geophys. Res.* 76:1954–66
Savage, J. C., Burford, R. O. 1973. Geodetic determination of relative plate motion in central California. *J. Geophys. Res.* 78: 832–45
Savage, J. C., Prescott, W. H. 1978. Comment on Melosh, 1976. *J. Geophys. Res.* 83:5005–7
Schapery, R. A. 1975. A theory of crack initiation and growth in viscoelastic media: I. theoretical development, *Int. J. Fract.* 11:141–59
Schmidt, R. A. 1976. Fracture-toughness testing of limestone. *Exp. Mech.* 16: 161–67
Schmidt, R. A. 1977. Fracture mechanics of oil shale–unconfined fracture toughness, stress corrosion cracking and tension test results. See Abou-Sayed 1977, pp. 2A2-1–2A2-6
Schmidt, R. A., Huddle, C. W. 1977. Effect of confining pressure on fracture toughness of Indiana limestone. *Int. J. Rock Mech. Min. Sci. Geomech. Abstr.* 14: 289–93
Schmidt, R. A., Lutz, T. J. 1979. *$K_{IC}$ and $J_{IC}$ of Westerly granite—effects of thickness and in-plane dimensions.* In *Fracture Mechanics Applied to Brittle Materials*, ed. S. W. Freiman, *ASTM Spec. Tech. Publ. 678*, pp. 166–82. Philadelphia: Am. Soc. Test. Mater.
Scholz, C. H. 1972. Static fatigue of quartz. *J. Geophys. Res.* 77:2104–14
Sieh, K. 1978a. Prehistoric large earthquakes produced by slip on the San Andreas fault at Pallett Creek, California. *J. Geophys. Res.* 83:3907–39
Sieh, K. 1978b. Central California foreshocks of the great 1857 earthquake. *Bull. Seismol. Soc. Am.* 68:1731–49
Simons, D. A. 1977. Boundary layer analysis of propagating mode II cracks in porous elastic media. *J. Mech. Phys. Solids* 25: 99–116
Steketee, J. A. 1958. Some geophysical applications of the elasticity theory of dislocations. *Can. J. Phys.* 36:1168–98
Stuart, W. D. 1979. Quasi-static earthquake mechanics. *Rev. Geophys. Space Phys.* 17: 1115–20
Stuart. W. D., Mavko, G. M. 1979. Earthquake instability on a strike-slip fault. *J. Geophys. Res.* 84:2153–60
Swanson, P. L., Spetzler, H. 1979. Stress corrosion of single cracks in flat plates of rock. *EOS, Trans. Am. Geophys. Union* 60:380
Swolfs, H. S. 1972. Chemical effects of pore fluids on rock properties. In *Underground Waste Management and Environmental Implications*, ed. T. D. Cook, pp. 224–34. *Am. Assoc. Petrol. Geol. Mem. 18*
Tada, H., Paris, P. C., Irwin, G. R. 1973.

*The Stress Analysis of Cracks Handbook.* Hellertown. Pa: Del Research Corp.
Tapponnier, P., Brace, W. F. 1976. Development of stress-induced microcracks in Westerly granite. *Int. J. Rock Mech. Min. Sci. Geomech. Abstr.* 13:103–12
Thatcher, W. 1979. Systematic inversion of geodetic data in Central California. *J. Geophys. Res.* 84:2283–95
Wachtman, J. B. 1974. Highlights of progress in the science of fracture of ceramics and glass. *J. Am. Ceram. Soc.* 57:509–19
Wawersik, W. R., Brace, W. F. 1971. Post failure behavior of a granite and a diabase. *Rock Mech.* 3:61–85
Weaver, J. 1977. Three-dimensional crack analysis. *Int. J. Solids Struct.* 13:321–30
Willis, J. R. 1967. A comparison of the fracture criteria of Griffith and Barenblatt, *J. Mech. Phys. Solids* 15:151–62
Wilkening, W. W. 1978. J-integral measurement in geological materials. See Kobayashi & Fourney 1978, pp. 254–58